Biosensors and Bioelectronics 143 (2019) 111593

Contents lists available at ScienceDirect

Biosensors and Bioelectronics

journal homepage: www.elsevier.com/locate/bios

Ultra-sensitive label-free electrochemical detection of the acute leukaemia gene Pax-5a based on enzyme-assisted cycle amplification

Weihua Zhao[a,1], Mingbin Liu[a,1], Hongbo Li[a,*], Suqin Wang[a,**], Shasha Tang[a], Rong-Mei Kong[b,***], Ruqin Yu[c,****]

[a] Key Laboratory of Functional Small Organic Molecule, Ministry of Education, College of Chemistry and Chemical Engineering, Jiangxi Normal University, Nanchang, 330022, PR China
[b] College of Chemistry and Chemical Engineering, Qufu Normal University, Qufu Shandong, 273165, PR China
[c] State Key Laboratory for Chemo/Biosensing and Chemometrics, College of Chemistry and Chemical Engineering Hunan University, Changsha, 410082, PR China

ARTICLE INFO

Keywords:
Enzyme-assisted cycle amplification
G-quadruplex/hemin complex
Electrochemical biosensor
Acute leukaemia

ABSTRACT

Accurate and sensitive detection of the Pax-5a gene is of great importance in the early diagnosis and prognosis of acute leukaemia. Herein, a label-free electrochemical sensing system was proposed for the detection of the acute leukaemia Pax-5a gene based on enzyme-assisted signal amplification to generate abundant G-quadruplex/hemin DNAzyme. The presence of Pax-5a can open the hairpin probe (HP), which acts as a template. Under the action of the restriction enzymes Nt.BbvCI and Klenow fragment polymerase, the target gene Pax-5a is cycled to open the HP; On the other hand, a large number of G-quadruplex sequences are produced. The resulting G-quadruplex sequence is capable of forming the G-quadruplex/hemin complex on the surface of the electrode in the presence of hemin. The ultrasensitive label-free electrochemical detection of Pax-5a can be realized via the G-quadruplex/hemin complex-catalysed reduction of H_2O_2, and the detection limit was estimated to be as low as 4.6 fM. In addition, the biosensor has good specificity and stability, and also has excellent detection capabilities in a complex substrate environment. Therefore, the sensor shows great potential in bioanalysis and clinical diagnosis.

1. Introduction

Cancer, as one of the larger public health problems in the world, is still a major disease that seriously endangers human life and health. Since changes in oncogenes and tumor suppressor genes are events at the level of nucleic acid molecules, nucleic acid detection is extremely important in the diagnosis and treatment of cancer (Cronin et al., 2004; Fan et al., 2019; Liu et al., 2018b; Nesvet et al., 2019). As one of the most common human malignant neoplastic diseases, acute lymphoblastic leukaemia (ALL) has the highest prevalence among children (Ranjbar et al., 2019). In the USA, approximately 3,000 to 4,000 people are diagnosed with ALL each year, two-thirds of whom are children between the ages 2 and 5 (Dores et al., 2012). Pax-5 is the only paired-box (PAX) family member found in the haematopoietic system, and it can be classified into Pax-5a, Pax-5b, Pax-5c, Pax-5d and Pax-5e. Among them, Pax-5a is the most important, and Pax-5 usually refers to Pax-5a (Zwollo et al., 1997). Pax-5 is very important for B-cell differentiation and development (Adams et al., 1992; Cozma et al., 2007; Delogu et al., 2006; Heltemes-Harris et al., 2011; Mikkola et al., 2002), and its abnormal expression can cause B lymphocytic leukaemia (Cobaleda et al., 2007; Mullighan et al., 2007; Nebral et al., 2008). The Pax-5 gene mutation has become a biomarker for the study of B lymphocytic leukaemia (Barbosa et al., 2018; Gu et al., 2019; Hirano et al., 2019). However, there are few studies on the detection of the variant Pax-5 gene and the expression of this gene in patients with clinical ALL (Nebral et al., 2008). Therefore, it is of great urgency and necessity to develop some effective methods for Pax-5 gene mutation detection.

The G-quadruplex, a special type of DNA secondary structure, was first proposed in 1962 (Gellert et al., 1962). The four guanine (G) bases are joined end to end to form a G-tetrad, and the adjacent G-tetrads

* Corresponding author. Tel.: + 86 079188120380.
** Corresponding author.
*** Corresponding author.
**** Corresponding author.
E-mail addresses: lihongbo112@126.com (H. Li), wangsuqin163@163.com (S. Wang), kongrongmei@126.com (R.-M. Kong), rqyu@hnu.edu.cn (R. Yu).
[1] These authors contributed equally to this work and should be considered co-first authors.

https://doi.org/10.1016/j.bios.2019.111593
Received 23 May 2019; Received in revised form 31 July 2019; Accepted 10 August 2019
Available online 14 August 2019
0956-5663/

further form a G-quadruplex by π-π stacking (Bochman et al., 2012). Recently, the G-quadruplex has been observed by an increasing number of scientists and has been applied in anticancer treatment (Balasubramanian et al., 2011; Collie and Parkinson, 2011; Monchaud and Teulade-Fichou, 2008). By binding to small molecules, G-quadruplex DNAzyme has the advantage of high stability and peroxidase-mimetic activity. Due to these advantages, G-quadruplex DNAzyme is widely used in electrochemical biosensors (Yuan et al., 2015), fluorescent biosensors (Ma et al., 2018a; Qiu et al., 2011), photoelectrochemical biosensors (Wang et al., 2015a), etc. The G-quadruplex/hemin complex formed by G-quadruplex binding to hemin possesses peroxidase catalytic activity and thus can be applied to the construction of electrochemical biosensors (Shi et al., 2016; Wang et al., 2014, 2015b). In general, electrochemical DNA biosensors usually have some certain limitations in signal generation; for example, an appropriate electroactive substance needs to be labelled, which may limit the detection sensitivity. Introducing appropriate signal amplification techniques to the development of electrochemical DNA biosensors is a very attractive approach for improving detection sensitivity. The generally used DNA signal amplification techniques include polymerase chain reaction (PCR) (Cronin et al., 2004; Li and Rothberg, 2004; Xu et al., 2015), rolling circle amplification (RCA) (Ji et al., 2012; Wang et al., 2011a, 2011b), restriction endonuclease-assisted signal amplification (Li et al., 2008; Xu et al., 2016), exonuclease III-assisted target recycling (Zuo et al., 2010) and hybridization chain reaction (HCR) (Huang et al., 2011; Wang et al., 2001). All these techniques have effectively improved the sensitivity of target DNA detection.

In this study, we proposed a label-free electrochemical DNA biosensor using restriction endonuclease-assisted signal amplification and successfully applied this biosensor for Pax-5a gene detection. The sensor contains three reactions. The first is a restriction endonuclease-assisted target recycling reaction that can produce a large number of G-rich sequences. The second reaction is to introduce the G-rich sequences onto the electrode surface, forming the G-quadruplex/hemin complex. The final reaction is the G-quadruplex/hemin complex-induced catalytic electrochemical reduction reaction of H_2O_2, which can produce a detectable electrochemical signal (He and Jiao, 2016; Meng et al., 2016; Yang et al., 2015). Because the restriction endonuclease-assisted signal amplification generates numerous G-quadruplex sequences, an improved sensitivity can be achieved for Pax-5a detection.

2. Experimental

2.1. Materials and reagents

Tris-HCl, tris-(2-carboxvethy)-phosphine hydrochloride (TCEP), 6-mercaptohexanol (MCH), hemin, hydrogen peroxide (H_2O_2), 4-(2-hydroxyethyl) piperazine-1 ethanesulfonic acid sodium salt (HEPES) and dimethyl sulfoxide (DMSO) were purchased from Aladdin Chemistry Co., Ltd. (Shanghai, China). Hemin stock solution (10 mM) was dissolved in DMSO and stored at −20 °C in the dark. The required concentration of hemin was obtained by dilution with 10 mM HEPES buffer (150 mM NaCl, 50 mM KCl, pH 7.2) before use. Deoxyribonucleoside triphosphates (dNTPs, 10 mM) were obtained from Takara Biotechnology Co., Ltd. (Dalian, China). Klenow fragment polymerase (3′–5′ exo-), Nt.BbvCI nicking endonuclease, 10 × NEB Buffer 2 (100 mM Tris-HCl, 500 mM NaCl, 100 mM $MgCl_2$, 10 mM dithiothreitol (DTT), pH 7.9), low molecular weight DNA ladder supplied with 10 × NEB Buffer 2, and 10 × CutSmart Buffer (200 mM Tris-HAc, 500 mM KAc, 100 mM $MgAc_2$, 1 g/mL BSA, pH 7.9) were obtained from New England Biolabs Inc. (Beijing, China). SYBR Green I was purchased from Dingguo Changsheng Biotechnology Co., Ltd. (Beijing, China). All solutions were prepared using Milli-Q water (18.4 MΩ).

All oligonucleotides were synthesized by Takara Biotechnology Co., Ltd. (Dalian, China), and the sequences are shown in Table S1.

2.2. Apparatus and measurements

Ultraviolet absorption spectroscopy was carried out on a UV-2700 spectrophotometer (Hitachi, Japan) for screening suitable primer sequences. A CHI760E electrochemical workstation (Shanghai Chenhua, China) was used for the electrochemical measurements. The traditional three-electrode system used in the experiment includes a modified working electrode (AuE, 1.6 mm in diameter), a saturated calomel electrode as a reference electrode, and a platinum wire auxiliary electrode. An $[Fe(CN)_6]^{3-/4-}$ solution containing 0.1 M KCl was used for cyclic voltammetry (CV) and electrochemical impedance spectroscopy (EIS) measurements. The CV voltage range was from −0.3 V to +0.7 V, and the sweep speed was 50 mV/s. The initial potential in EIS was 0.23 V, and the scanning frequency ranged from 0.1 Hz to 10000 Hz. Differential pulse voltammetry (DPV) measurements were performed in 20 mM HEPES buffer with a potential range from −0.15 to −0.5 V and a pulse amplitude of 50 mV.

2.3. Polyacrylamide gel electrophoresis (PAGE)

PAGE (12%) was performed to investigate the feasibility of the proposed biosensor. Each group of samples was prepared according to experimental procedures. Then, the reaction solution was mixed with 10 × SYBR Green I and 6 × loading buffer for 10 min at room temperature. Finally, the above solution was injected into the PAGE well to perform gel electrophoresis in 0.5 × TBE buffer at room temperature for 90 min (voltage = 90 V). The gel was photographed with a ChemiDoc XRS chemiluminometer (Bio-Rad, USA).

2.4. Electrode modification

First, the TP was treated with TCEP (2 mM, 10 mM Tris-HCl) at 37 °C for 2 h to reduce the disulfide bonds present. Then, 10 μL of the pretreated TP solution (0.3 μM) was dropped onto the AuE surface and incubated at 4 °C overnight. After the AuE was rinsed with Tris-HCl buffer (10 mM, 1 mM EDTA) to remove the unbound Thiolated Probe (TP), 2 mM MCH was used to react with the electrode to remove the nonspecifically adsorbed DNA. Finally, the obtained TP/MCH/AuE sensing surface was thoroughly rinsed with 10 mM Tris-HCl buffer and used for the next reaction.

2.5. Enzyme-assisted recycling amplified detection of Pax-5a

The HP was first annealed at 90 °C for 5 min and slowly cooled down to room temperature. Next, 2 μL of 10 μM HP and 1 μL of Pax-5a solutions at different concentrations (final concentration range from 0 to 500 pM) were added to a mixture containing 1 × NEB Buffer 2 and 1 × CutSmart Buffer for 1 h at 37 °C. Subsequently, 2 μL of 10 μM Primer 4 (P4), 0.4 μL of 5 U/μL Klenow fragment (3′-5′ exo-), 1 μL of 10 mM dNTPs and 1 μL of 10 U/μL Nt.BbvCI nickase were added to the resulting solution and incubated at 37 °C for 3 h to achieve enzyme-assisted recycling amplification. The resulting solution was heated at 80 °C for 20 min to inactivate the enzymes.

Then, the above solution was transferred onto the HP/MCH/AuE sensing surface. After incubating at 37 °C for 60 min, the AuE was rinsed with 10 mM Tris-HCl, and then 10 μL of 20 μM hemin was dropped onto the electrode surface and reacted at 37 °C for 60 min to form the G-quadruplex/hemin complex. Finally, DPV measurements were carried out in 10 mM HEPES buffer containing 3 mM H_2O_2.

3. Results and discussion

3.1. Detection principle

Scheme 1 describes the principle of Pax-5a gene detection using an enzymatic signal amplification-based electrochemical biosensor. First,

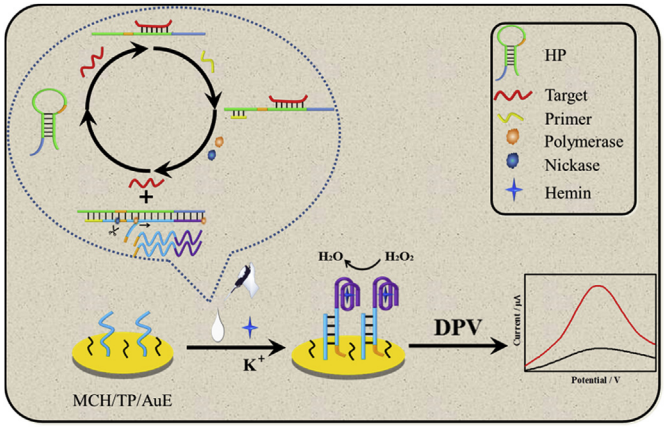

Scheme 1. Schematic illustration of the enzymatic signal amplification-based electrochemical biosensor for the detection of the Pax-5a gene.

the stem-loop structure of the hairpin probe (HP) was opened via hybridization with the target Pax-5a gene, triggering further hybridization of the opened HP with the primer (P4). The 3′ segment of P4 can be extended by the HP as a template under the action of a polymerase. In this process, double-stranded DNA containing the recognition site of the restriction endonuclease Nt.BbvCI was formed, and Pax-5a was replaced simultaneously to combine with another HP to initiate the next cycle of chain replacement polymerization. Nt.BbvCI is a restriction endonuclease that can recognize a specific double-stranded DNA fragment, (5′-CCTCAGC-3′/3′-GGAGTCG-5′), but cleaves only one specific strand (Wen et al., 2012). Using this property, a large number of G-rich sequences on the newly generated duplex were replaced by the continuous alternating action of the polymerase and the endonuclease. Then, the above reaction solution containing the generated G-rich sequences was dropped onto the surface of the modified AuE to hybridize with the TP. Finally, the introduction of hemin and K^+ induced the formation of G-quadruplex/hemin complexes, which can act as an electrocatalytic label. Since the enzymatic amplification generated a large number of G-rich sequences, ultrasensitive detection of Pax-5a can be realized via the G-quadruplex/hemin complex-catalysed electrochemical reduction of H_2O_2 (Han et al., 2017).

3.2. Characterizations of the biosensor

The stepwise preparation of the biosensor was confirmed by performing CV and EIS measurements in an $[Fe(CN)_6]^{3-/4-}$ solution containing 0.1 M KCl. As shown in Fig. 1A, the voltammogram of the bare AuE (curve a) shows a well-defined redox peak. A significant decrease in redox current and an increase in peak separation (curve b) were observed, possibly due to electrostatic repulsion between $[Fe(CN)_6]^{3-/4-}$ and the negative DNA backbone of the immobilized TP (Patolsky et al., 1999). After binding of the G-rich sequence by TP, G-quadruplex/hemin complexes were formed in the presence of K^+ and hemin, resulting in a further reduced current response (curve c) due to the introduction of a large number of negative charges onto the electrode surface. Fig. 1B shows the changes in the EIS spectrum at various stages of the electrode modification process. The diameter of the semicircle indicates the magnitude of the charge transfer resistance of the electrode surface (Rct). The bare AuE exhibits a very small semicircular diameter (curve a, Rct = 260 Ω), indicating a very small impedance intensity. After immobilizing the TP onto the AuE surface and blocking with MCH, the radius of the semicircular domain increases (curve b, about 525 Ω) due to the increased charge transfer resistance. After the G-rich sequence binds to the TP on the AuE surface and forms the G-quadruplex/hemin complex, a larger semicircle (curve c, Rct = 1144 Ω) was observed. This behaviour is because the formed G-quadruplex/hemin complex has a more ordered and denser accumulation on the electrode surface than

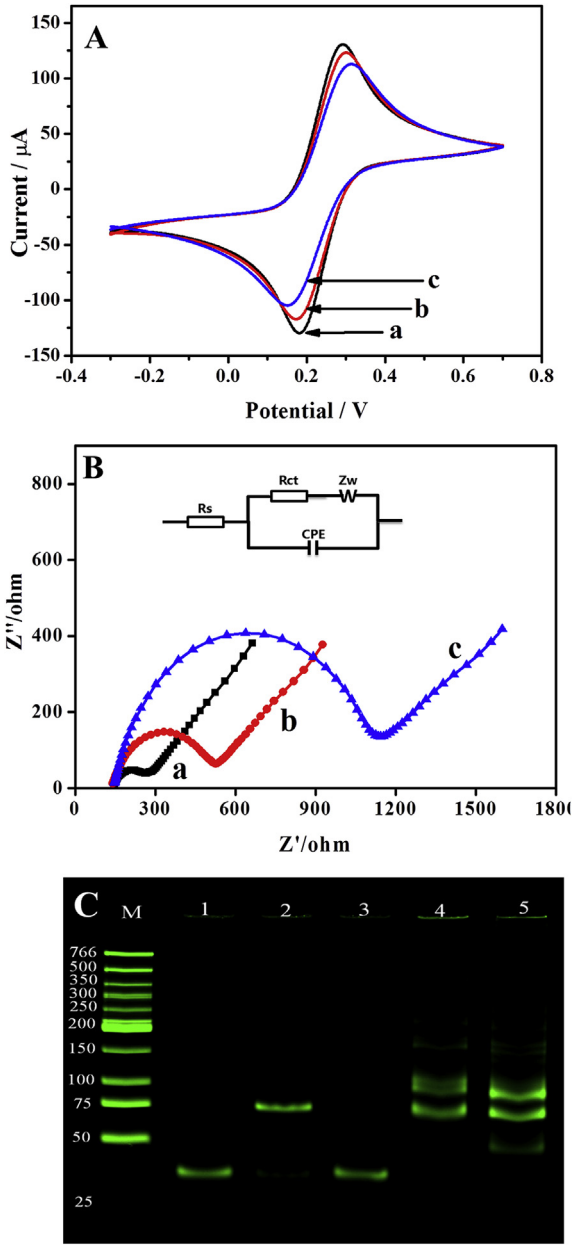

Fig. 1. CV (A) and EIS (B) measurements of the electrodes in different modification stages. (a) Bare AuE, (b) TP/MCH/AuE, and (c) the formation of the G-quadruplex/hemin complex. The CV and EIS experiments were performed in 5 mM $[Fe(CN)6]^{3-/4-}$ containing 0.1 M KCl. (C) PAGE analysis. M. Markers; 1. HP; 2. HP and Pax-5a; 3. HP and Primer 4; 4. HP, Pax-5a, Primer 4, Klenow fragment and Nt.BbvCI; 5. HP, Pax-5a, Primer 4, Klenow fragment, Nb.BbvCI and TP. [HP] = 0.5 μM, [Pax-5a] = 0.25 μM, [P4] = 0.5 μM, [TP] = 0.5 μM, [Klenow fragment] = 50 U/mL, [Nt.BbvCI] = 250 U/mL.

the G-rich sequence, resulting in stronger repulsion of the negatively charged redox species (Yang et al., 2012). These results confirmed the successful manufacture of the electrochemical biosensor.

To further characterize the construction of the proposed biosensor, we performed PAGE analysis (Fig. 1C). By comparing lane 2 and lane 3, one can obviously observe the hybridization product between the HP and the target Pax-5a gene. A fully complementary high molecular weight hybrid duplex and a large number of G-rich single strands (lane 4) were generated by the action of the polymerase Klenow fragment and the endonuclease Nb.BbvCI. Upon further addition of the TP, a slightly lower molecular weight hybridization product of the G-rich sequence and TP appeared. The results of the gel experiments showed

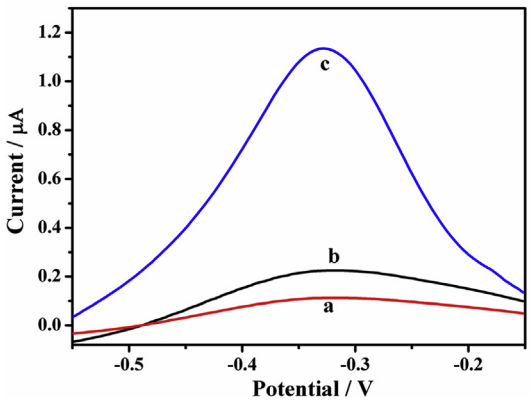

Fig. 2. DPV responses of (a) TP/MCH/AuE, (b) TP/MCH/AuE incubated with mixed reaction solution without the target and (c) TP/MCH/AuE incubated with G-quadruplex/hemin complex solution including the target Pax-5a gene (100 pM). [HP] = 0.5 μM, [P4] = 0.5 μM, [TP] = 0.3 μM, [Klenow fragment] = 50 U/mL, [Nt.BbvCI] = 250 U/mL.

that the biosensors were capable of detecting the target DNA.

3.3. Feasibility investigation of electrochemical detection

To prove that the designed sensor can effectively detect the target gene, we used DPV to detect samples of different compositions. The result is shown in Fig. 2. Compared to the very small DPV peak, which is almost identical to the DPV peak of the modified TP/MCH/AuE electrode (curve a), the DPV peak observed after incubation with the reaction solution without target DNA (curve b) exhibits a weak increase. This effect may be due to the enzymatic amplification resulting in the nonspecific generation of G-rich sequences, thus increasing the background peak current. However, in the presence of Pax-5a, a significant increase in the DPV peak (curve c) is observed near −0.35 V. Since the G-quadruplex/hemin complex can catalyze the oxidation of ABTS by H_2O_2, UV absorption spectroscopy can also be used to verify the successful manufacture of the sensor. The UV absorption spectrum is shown in Fig. S2. When the target gene is absent, the absorption peak (curve b) is close to the absorption peak of the blank reference (curve a). When the target gene Pax-5a was added, a significant ultraviolet absorption peak (curve c) appeared. The signal response of the electrochemical biosensor with the increasing concentration of H_2O_2 was studied by i-t curve, and the result is shown in Fig. S3. These results indicate that the successful preparation of electrochemical biosensors and can potentially be applied to the electrochemical detection of the Pax-5a gene.

3.4. Analytical performance of the biosensors

According to the optimal reaction conditions obtained in Fig. S1, the DPV signals for target DNA with different concentrations were measured to evaluate the sensitivity of the designed biosensor. In Fig. 3A, the DPV peak current increases as the target DNA concentration increases in the range from 0 to 10 nM. Fig. 3B shows that there is a good linear relationship between the DPV peak current (−0.35 V) and target DNA concentration in the range from 10 fM to 500 pM, with a linear regression equation of $i = 0.1994\lg c + 3.1232$ ($R^2 = 0.9910$), the c represents the concentration of Pax-5a. Based on the 3σ/slope rule, the detection limit is estimated to be 4.6 fM, indicating that ultrasensitive detection of Pax-5a can be achieved using the developed biosensor. Moreover, the sensing performance of the electrochemical Pax-5a gene biosensor was compared with other previously reported DNA sensing systems and detection methods (Table 1). The results indicated that the sensitivity of the developed electrochemical Pax-5a gene biosensor is comparable or superior to that of most other reported DNA biosensors.

3.5. Specificity of the biosensor

The sequence specificity of the proposed electrochemical Pax-5a gene biosensor was investigated by comparing the DPV responses induced by DNA sequences containing single-base (MT1), two-base (MT2), three-base (MT3) and non-complementary DNA (Non) with that induced by the target Pax-5a gene. As shown in Fig. 4A, compared to the blank solution, both MT1 and MT2 induced very small current responses, while MT3 and Non caused almost no signal changes. These results indicated a high sequence specificity for the target DNA owing to the impaired ability of the mismatched DNA to open the unique stem-loop structure of the HP. This property results in a reduction in the generation of the enzymatic amplification product G-rich sequences and thus a reduction in G-quadruplex/hemin complexes. Therefore, a significant decrease in the DPV response can be observed.

In addition, we also conducted a control experiment with the HP. Verification of the correctness of the designed HP sequence was conducted by changing the sequence of the G-rich region of HP, and the result is shown in Fig. 4B. The current response of the control group was almost equal to the current response of the blank control group. The DPV peaks in these groups were much smaller than those in the experimental group. This finding proves that the hairpin we designed is correct. In addition, the effect of protein adsorption on electrochemical sensors was investigated. The result is shown in Fig. S4. As can be seen from the Fig. S4, protein adsorption can interfere with the measurement of the electrodes. However, the enzymatic amplification reaction is carried out outside the electrode in this work. And it is effective to avoid these interferences.

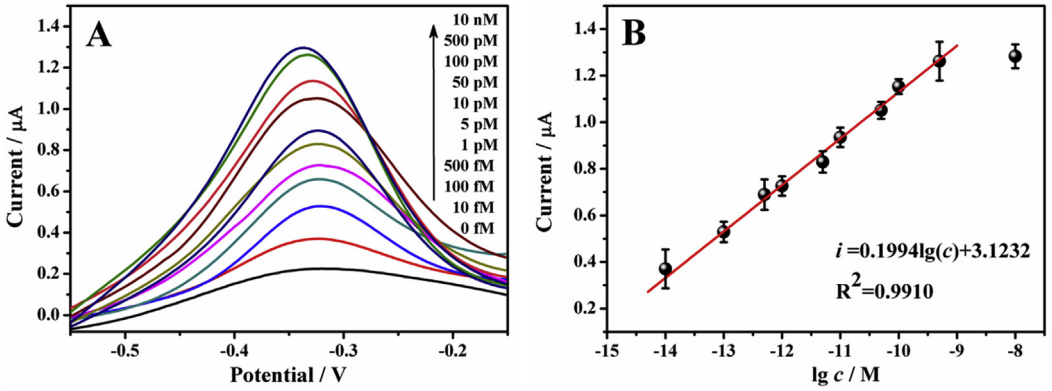

Fig. 3. (A) The typical DPV responses of the biosensor to different concentrations of the target Pax-5a from 0 fM to 500 pM. (B) The corresponding calibration plot for the DPV peak current *vs.* lg*c*. Error bars, SD, n = 3. [HP] = 0.5 μM, [P4] = 0.5 μM, [TP] = 0.3 μM, [Klenow fragment] = 50 U/mL, [Nb.BbvCI] = 250 U/mL.

Table 1
Comparison of various target DNA detection methods.

Analysis method	Detection technique	Linear range	LOD	Reference
ISDA sensing system	Fluorescence	10 pM - 150 nM	10 pM	Li et al. (2019)
Novel cascade PEC	Photoelectrochemistry	1 pM - 50 nM	0.76 pM	Wen et al. (2017)
Co-sensitized structure DNA sensor	Photoelectrochemistry	10 fM - 0.1 μM	3 fM	Liu et al. (2018a)
Dual-signal ratiometric	Electrochemistry	0.02 pM - 2 nM	12.8 fM	Ma et al. (2018b)
EATR	Electrochemistry	0.1 pM - 1 μM	42 fM	Wang et al. (2017)
TSDR and cruciform DNA crystal	Electrochemistry	1 pM - 100 nM	0.21 pM	Hu et al. (2018)
NESA	Electrochemistry	1 pM–10 pM	0.35 pM	Tan et al. (2015)
Enzyme-assisted amplification	Electrochemistry	10 fM - 500 pM	4.6 fM	This work

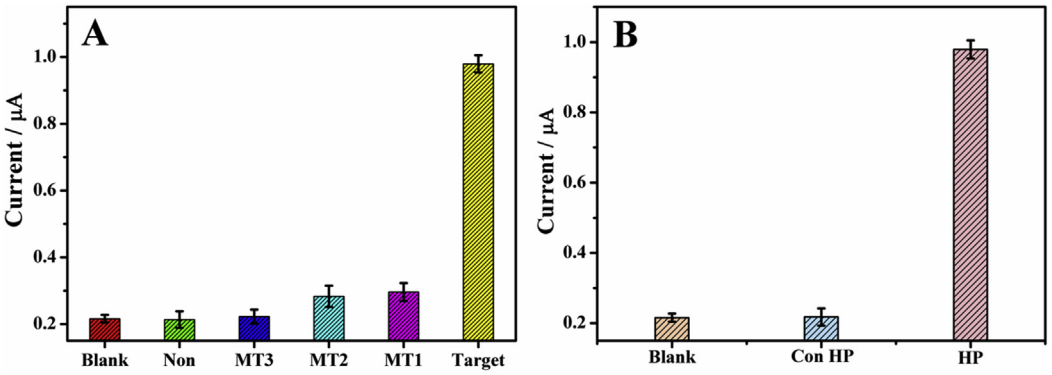

Fig. 4. (A) Selectivity investigation and (B) control experiment of the proposed biosensor. [HP] = [Con HP] = 0.5 μM, [P4] = 0.5 μM, [TP] = 0.3 μM, [Klenow fragment] = 50 U/mL, [Nb.BbvCI] = 250 U/mL. The concentrations of MT1, MT2, MT3 and Non are all 500 pM.

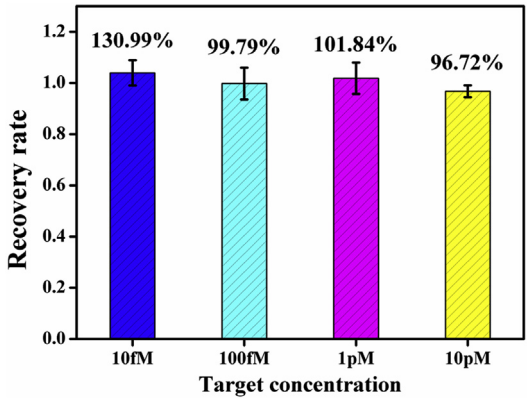

Fig. 5. Recovery experiments for different target DNA concentrations of the biosensor (n = 3). [HP] = 0.5 μM, [P4] = 0.5 μM, [TP] = 0.3 μM.

3.6. Biosensor applicability

To assess the effectiveness of our proposed biosensors in detecting the target DNA in complex biological matrices, we designed recovery experiments for different target DNA concentrations. Different concentrations of Pax-5a (10 fM, 100 fM, 1 pM and 10 pM) were added to the B lymphocyte lysate sample solution and diluted with 1 × NEB Buffer 2. As shown in Fig. 5, the recoveries ranged from 96.73% to 103.99% and the RSD values ranged from 2.4% to 6.2%, which indicating that the designed sensor is satisfactory and has potential applications for detecting Pax-5a in complex biological substrate environments.

We also investigated the stability of biosensors. Six electrodes were independently fabricated under the same conditions, and DPV measurements were taken after storage for 0, 2, 4, 6, 8, and 10 days at 4 °C, respectively. The result is shown in Fig. S5. Typical DPV responses were 1.119 μA, 1.118 μA, 1.11 μA, 1.09 μA, 1.07 μA, and 1.06 μA, respectively. The results show that at least 95% of the response of the biosensor to the target gene is still present, indicating that the sensor has good storage stability.

4. Conclusions

In summary, a signal-amplified electrochemical biosensor based on an enzyme-assisted target cycle for label-free detection of the Pax-5a gene was successfully developed. That is to say, an enzyme-assisted circular signal amplification strategy, using polymerase to control DNA transcription and restriction endonuclease to cleave the specific site of DNA, was performed to achieve ultrasensitive detection of Pax-5a gene, and the LOD could be as low as 4.6 fM. The sensor has excellent selectivity and stability, and can successfully detect the Pax-5a gene in a spiked complex matrix. In addition, it is noteworthy that the proposed enzymatic amplification reaction of the electrochemical biosensor is carried out outside the electrode, which improves the reaction efficiency and reduces the complexity of the operation. At the same time, the detection interference caused by the adsorption of substances (including nucleic acid strands and enzyme proteins, etc.) in each step of the electrode surface reaction is also avoided. Thus, the biosensor with these advantages can provide a promising platform for the early diagnosis and research of B lymphocytic leukemia.

CRediT authorship contribution statement

Weihua Zhao: Data curation, Formal analysis. **Mingbin Liu:** Data curation, Formal analysis. **Hongbo Li:** Conceptualization, Funding acquisition, Writing - original draft, Writing - review & editing. **Suqin Wang:** Conceptualization, Funding acquisition, Writing - original draft, Writing - review & editing. **Shasha Tang:** Data curation, Formal analysis. **Rong-Mei Kong:** Conceptualization, Funding acquisition, Writing - original draft, Writing - review & editing. **Ruqin Yu:** Conceptualization, Funding acquisition, Writing - original draft, Writing - review & editing.

Acknowledgements

This work was supported by the National Natural Science Foundation of China (NSFC) (Grant No: 21565015, 21663014); the Foundation of Jiangxi Educational Committee (GJJ150363); the State Key Laboratory of Chemical Biosensing & Chemometrics (Z2015022); and the Key Laboratory of Functional Small Organic Molecules (KLFS-KF-201425).

Appendix A. Supplementary data

Supplementary data to this article can be found online at https://doi.org/10.1016/j.bios.2019.111593.

References

Adams, B., DC6rfler, P., Aguzzi, A., Kozmik, Z., UrbC!nek, P., Maurer-Fogy, I., Busslinger, M., 1992. Genes Dev. 6 (9), 1589–1607.
Balasubramanian, S., Hurley, L.H., Neidle, S., 2011. Nat. Rev. Drug Discov. 10, 261.
Barbosa, T.C., Lopes, B.A., Blunck, C.B., Mansur, M.B., Deyl, A.V.S., Emerenciano, M., Pombo-de-Oliveira, M.S., 2018. BMC Med. Genomics 11 (1), 122.
Bochman, M.L., Paeschke, K., Zakian, V.A., 2012. Nat. Rev. Genet. 13, 770.
Cobaleda, C.C.s., Schebesta, A., Delogu, A., Busslinger, M., 2007. Nat. Immunol. 8, 463.
Collie, G.W., Parkinson, G.N., 2011. Chem. Soc. Rev. 40 (12), 5867–5892.
Cozma, D., Yu, D., Hodawadekar, S., Azvolinsky, A., Grande, S., Tobias, J.W., Metzgar, M.H., Paterson, J., Erikson, J., Marafioti, T., Monroe, J.G., Atchison, M.L., Thomas-Tikhonenko, A., 2007. J. Clin. Invest. 117 (9), 2602–2610.
Cronin, M., Pho, M., Dutta, D., Stephans, J.C., Shak, S., Kiefer, M.C., Esteban, J.M., Baker, J.B., 2004. Am. J. Pathol. 164 (1), 35–42.
Delogu, A., Schebesta, A., Sun, Q., Aschenbrenner, K., Perlot, T., Busslinger, M., 2006. Immunity 24 (3), 269–281.
Dores, G.a.M., Devesa, S.S., Curtis, R.E., Linet, M.S., Morton, L.M., 2012. Blood 119 (1), 34.
Fan, J., Tong, C., Dang, W., Qin, Y., Liu, X., Liu, B., Wang, W., 2019. Talanta 204, 20–28.
Gellert, M., Lipsett, M.N., Davies, D.R., 1962. Proc. Natl. Acad. Sci. U. S. A. 48 (12), 2013–2018.
Gu, Z., Churchman, M.L., Roberts, K.G., Moore, I., Zhou, X., Nakitandwe, J., Hagiwara, K., Pelletier, S., Gingras, S., Berns, H., Payne-Turner, D., Hill, A., Iacobucci, I., Shi, L., Pounds, S., Cheng, C., Pei, D., Qu, C., Newman, S., Devidas, M., Dai, Y., Reshmi, S.C., Gastier-Foster, J., Raetz, E.A., Borowitz, M.J., Wood, B.L., Carroll, W.L., Zweidler-McKay, P.A., Rabin, K.R., Mattano, L.A., Maloney, K.W., Rambaldi, A., Spinelli, O., Radich, J.P., Minden, M.D., Rowe, J.M., Luger, S., Litzow, M.R., Tallman, M.S., Racevskis, J., Zhang, Y., Bhatia, R., Kohlschmidt, J., MrC3zek, K., Bloomfield, C.D., Stock, W., Kornblau, S., Kantarjian, H.M., Konopleva, M., Evans, W.E., Jeha, S., Pui, C.-H., Yang, J., Paietta, E., Downing, J.R., Relling, M.V., Zhang, J., Loh, M.L., Hunger, S.P., Mullighan, C.G., 2019. Nat. Genet. 51 (2), 296–307.
Han, C., Li, R., Li, H., Liu, S., Xu, C., Wang, J., Wang, Y., Huang, J., 2017. Microchim. Acta 184 (8), 2941–2948.
He, Y., Jiao, B., 2016. Microchim. Acta 183 (12), 3303–3309.
Heltemes-Harris, L.M., Willette, M.J.L., Ramsey, L.B., Qiu, Y.H., Neeley, E.S., Zhang, N., Thomas, D.A., Koeuth, T., Baechler, E.C., Kornblau, S.M., Farrar, M.A., 2011. J. Exp. Med. 208 (6), 1135.
Hirano, D., Hayakawa, F., Yasuda, T., Tange, N., Yamamoto, H., Kojima, Y., Morishita, T., Imoto, N., Tsuzuki, S., Mano, H., Naoe, T., Kiyoi, H., 2019. Oncogene 38 (13), 2263–2274.
Hu, Y., Li, H., Li, J., 2018. J. Electroanal. Chem. 822, 66–72.
Huang, J., Wu, Y., Chen, Y., Zhu, Z., Yang, X., Yang, C.J., Wang, K., Tan, W., 2011. Angew. Chem. Int. Ed. 50 (2), 401–404.
Ji, H., Yan, F., Lei, J., Ju, H., 2012. Anal. Chem. 84 (16), 7166–7171.
Li, Rothberg, L.J., 2004. JACS 126 (35), 10958–10961.
Li, H., Tang, Y., Zhao, W., Wu, Z., Wang, S., Yu, R., 2019. Anal. Chim. Acta 1065, 98–106.
Li, J.J., Chu, Y., Lee, B.Y.-H., Xie, X.S., 2008. Nucleic Acids Res. 36 (6) e36-e36.
Liu, X.-P., Chen, J.-S., Mao, C.-j., Niu, H.-L., Song, J.-M., Jin, B.-K., 2018a. Biosens. Bioelectron. 116, 23–29.
Liu, Y., Chen, X., Ma, Q., 2018b. Biosens. Bioelectron. 117, 240–245.
Ma, L., Han, X., Xia, L., Kong, R.M., Qu, F., 2018a. Analyst 143 (22), 5474–5480.
Ma, R., Wang, L., Wang, H., Jia, L., Zhang, W., Shang, L., Xue, Q., Jia, W., Liu, Q., Wang, H., 2018b. Sens. Actuators B Chem. 269, 173–179.
Meng, Y., Hun, X., Zhang, Y., Luo, X., 2016. Microchim. Acta 183 (11), 2965–2971.
Mikkola, I., Heavey, B., Horcher, M., Busslinger, M., 2002. Science 297 (5578), 110.
Monchaud, D., Teulade-Fichou, M.-P., 2008. Org. Biomol. Chem. 6 (4), 627–636.
Mullighan, C.G., Goorha, S., Radtke, I., Miller, C.B., Coustan-Smith, E., Dalton, J.D., Girtman, K., Mathew, S., Ma, J., Pounds, S.B., Su, X., Pui, C.-H., Relling, M.V., Evans, W.E., Shurtleff, S.A., Downing, J.R., 2007. Nature 446, 758.
Nebral, K., Denk, D., Attarbaschi, A., Kc6nig, M., Mann, G., Haas, O.A., Strehl, S., 2008. Leukemia 23, 134.
Nesvet, J., Rizzi, G., Wang, S.X., 2019. Biosens. Bioelectron. 124–125, 136–142.
Patolsky, F., Katz, E., Bardea, A., Willner, I., 1999. Langmuir 15 (11), 3703–3706.
Qiu, B., Zheng, Z.-Z., Lu, Y.-J., Lin, Z.-Y., Wong, K.-Y., Chen, G.-N., 2011. Chem. Commun. 47 (5), 1437–1439.
Ranjbar, R., Karimian, A., Aghaie Fard, A., Tourani, M., Majidinia, M., Jadidi-Niaragh, F., Yousefi, B., 2019. J. Cell. Physiol. 234 (4), 3216–3230.
Shi, K., Dou, B., Yang, J., Yuan, R., Xiang, Y., 2016. Anal. Chim. Acta 916, 1–7.
Tan, Y., Wei, X., Zhao, M., Qiu, B., Guo, L., Lin, Z., Yang, H.-H., 2015. Anal. Chem. 87 (18), 9204–9208.
Wang, F., Elbaz, J., Orbach, R., Magen, N., Willner, I., 2011a. JACS 133 (43), 17149–17151.
Wang, F., Elbaz, J., Teller, C., Willner, I., 2011b. Angew. Chem. Int. Ed. 50 (1), 295–299.
Wang, G.L., Shu, J.X., Dong, Y.M., Wu, X.M., Zhao, W.W., Xu, J.J., Chen, H.Y., 2015a. Anal. Chem. 87 (5), 2892–2900.
Wang, J., Polsky, R., Xu, D., 2001. Langmuir 17 (19), 5739–5741.
Wang, Q., Yang, C., Xiang, Y., Yuan, R., Chai, Y., 2014. Biosens. Bioelectron. 55, 266–271.
Wang, S., Yang, F., Jin, D., Dai, Q., Tu, J., Liu, Y., Ning, Y., Zhang, G.J., 2017. Anal. Chem. 89 (10), 5349–5356.
Wang, X., Jiang, A., Hou, T., Li, F., 2015b. Anal. Chim. Acta 890, 91–97.
Wen, G., Yang, X., Wang, Y., 2017. J. Mater. Chem. B 5 (37), 7775–7780.
Wen, Y., Xu, Y., Mao, X., Wei, Y., Song, H., Chen, N., Huang, Q., Fan, C., Li, D., 2012. Anal. Chem. 84 (18), 7664–7669.
Xu, J., Wu, Z.-S., Shen, W., Xu, H., Li, H., Jia, L., 2015. Biosens. Bioelectron. 73, 19–25.
Xu, J., Wu, Z.-S., Wang, Z., Li, H., Le, J., Jia, L., 2016. Biomaterials 100. pp. 110–117.
Yang, J., Xiang, Y., Song, C., Liu, L., Jing, X., Xie, G., Xiang, H., 2015. Microchim. Acta 182 (15), 2377–2385.
Yang, N., Cao, Y., Han, P., Zhu, X., Sun, L., Li, G., 2012. Anal. Chem. 84 (5), 2492–2497.
Yuan, L., Tu, W., Bao, J., Dai, Z., 2015. Anal. Chem. 87 (1), 686–692.
Zuo, X., Xia, F., Xiao, Y., Plaxco, K.W., 2010. JACS 132 (6), 1816–1818.
Zwollo, P., Arrieta, H., Ede, K., Molinder, K., Desiderio, S., Pollock, R., 1997. J. Biol. Chem. 272 (15), 10160–10168.